MNT suppresses T cell apoptosis via BIM and is vital for MYC-driven T lymphomagenesis

Hai Vu Nguyen
Walter and Eliza Hall Institute of Medical Research https://orcid.org/0000-0001-6974-1630
Cassandra J Vandenberg
Walter and Eliza Hall Institute of Medical Research https://orcid.org/0000-0002-8891-8873
Mikara R Robati
Walter and Eliza Hall Institute of Medical Research
Ashley P Ng
Walter and Eliza Hall Institute of Medical Research https://orcid.org/0000-0001-9690-0879
Suzanne Cory (cory@wehi.edu.au)
Walter and Eliza Hall Institute of Medical Research https://orcid.org/0000-0002-6818-3451

Research Article

Keywords: MYC, MNT, BIM, apoptosis, T lymphomagenesis, T lymphopoiesis, transgenic mice

Posted Date: April 15th, 2022

DOI: https://doi.org/10.21203/rs.3.rs-1555936/v1

Abstract

The importance of c-MYC in regulating normal lymphopoiesis and promoting lymphomagenesis is well-established, but far less appreciated is the vital supporting role of MYC's relative MNT. We show here that, during normal T cell development, MNT loss enhances apoptosis and establish the mechanism as elevated expression of the pro-apoptotic BH3-only protein BIM. Using a *MYC* transgenic mouse model, we also show that MNT loss reduces the pool of premalignant MYC-driven T cells and totally abrogates thymic T lymphomagenesis. Taken together with our recent demonstration that MNT is vital for the survival of MYC-driven premalignant and malignant B lymphoid cells, these results suggest that MNT represents an important new drug target for both T and B lymphoid malignancies.

Introduction

The transcription factor c-MYC (hereafter MYC) controls expression of many genes involved in the proliferation, growth, metabolism and DNA damage responses of normal cells in adult tissues [1, 2] and its deregulated overexpression is widely accepted as a major driver of human cancer [3, 4]. Importantly, under conditions of stress (e.g. cytokine or nutrient deprivation), cells expressing elevated MYC undergo apoptosis [5, 6, 7], and this serves as a critical restraint on neoplastic transformation. Hence, genetic defects that impede apoptosis boost MYC's oncogenic potential, as first revealed by the seminal demonstration that anti-apoptotic BCL-2 synergises with MYC in lymphomagenesis [8, 9].

To activate transcription, MYC heterodimerises with MAX, another ubiquitously expressed basic Helix-Loop-Helix Leucine Zipper (bHLHLZ) protein, and together they bind E-box motifs (CACGTG) in target genes [1]. However, MAX also binds several MYC-related transcriptional repressors containing bHLHLZ domains [1, 10]. MNT, an important member of this MXD (MAX Dimerization) family of c-MYC antagonists [11, 12, 13] is essential for embryonic development [14] and widely expressed in mammalian tissues.

We recently showed that MNT is vital for B lymphomagenesis in Eμ-*Myc* transgenic mice [15], which model human Burkitt's lymphoma [16]. We found that MNT aids MYC by suppressing apoptosis in both premalignant MYC-driven pre-B cells and fully malignant B lymphoid tumour cells.

Human T cell malignancies are associated with a very poor prognosis and new therapeutic approaches are sorely needed [17, 18]. Here, building on earlier studies [19, 20, 21], we investigate how MNT loss impacts normal T cell development and T lymphomagenesis. We confirm that MNT loss promotes T cell apoptosis and provide new genetic and biochemical evidence regarding the underlying mechanism. We also establish, for the first time, that MNT loss reduces the competitive fitness of both T and B lymphopoiesis. We show that MNT loss prevents T lymphoma development, and elucidate the cause by dissecting T cell development in young MNT-null *MYC* transgenic mice. Taken together, these studies indicate that MNT can facilitate MYC-driven tumorigenesis rather than acting as a tumour suppressor as

previously suggested [4, 22, 23, 24]. The results have important therapeutic implications for MYC-driven T and B lymphoid tumours and perhaps many other MYC-driven tumour types.

Materials And Methods

Mice

Mice used were *Mnt*$^{fl/fl}$ [22], *Rag1Cre* [25], *MYC10*^{hom} [26] and *Bim*$^{-/-}$del339 [27], all on a C57BL/6 background. Note that homozygous *Mnt* deletion, initially reported as perinatal lethal [14], is fatal at ~ E10 in C57BL/6 mice bred in our facility [15]. Breeding, genotyping and phenotype analyses are detailed in Supplementary Materials and Methods.

Competitive bone marrow repopulation

C57BL/6 mice (Ly5.1$^+$) were lethally irradiated (2 x 550 Rad) and reconstituted with 10^6 bone marrow cells from C57BL/6 mice (Ly5.1$^+$ competitor cells) and 10^6 bone marrow cells from either *Mnt*$^{+/+}$*Rag1Cre* or *Mnt*$^{fl/fl}$*Rag1Cre* mice (Ly5.2$^+$ test cells). Twelve weeks after transplantation, the relative proportions of test- and competitor-derived cells in the thymus, spleen and bone marrow of recipients was determined by flow cytometry, using CD45.1 and CD45.2 antibodies to distinguish Ly5.1$^+$ and Ly5.2$^+$ cells respectively.

OP9-DL1 co-culture

DN3 and DN4 T progenitor cells sorted from thymi of *Mnt*$^{+/+}$*Rag1Cre* and *Mnt*$^{fl/fl}$ *Rag1Cre* mice using a-CD4, a-CD8, a-CD25 and a-CD44 antibodies (see Supplementary Fig. S1) were cultured at 37^{o}C in 6-well plates containing a confluent monolayer of (unirradiated) OP9 cells expressing Notch ligand Delta-like 1 (OP9-DL1) [28] in the presence of 5ng/mL recombinant murine IL-7 for 3–4 d, after which lymphoid cells were recovered via a 40 micron cell strainer.

Statistical analysis

Statistical comparisons were made using unpaired two-tailed Student's *t*-test or ANOVA with Prism v8.0 software (GraphPad, San Diego, CA, USA). Data are shown as means ± SEM with *P*-values ≤ 0.05 considered statistically significant. Mouse survival analysis was carried out using GraphPad Prism (Version 8.0) and significance determined using log-rank (Mantel-Cox) test.

Results

Impact of MNT loss on T lymphopoiesis.

In adult mice, c-MYC is essential for normal T cell development and immune responses, regulating proliferative bursts in both the thymus and spleen [29, 30, 31, Mingueneau, 2013 #21545]. To ascertain MNT's role in T cell development, we crossed *Mnt*$^{fl/fl}$ mice [22] with *Rag1Cre* mice [25] and analysed the cellular composition of the thymus and spleen in 6–7 week-old offspring of each genotype. *Mnt* deletion

mediated via the *Rag1Cre* transgene, which is expressed only in early lymphoid progenitors [25], was very efficient, as shown by PCR and western blot analysis of the major thymic sub-populations (Fig. 1A).

Thymic weight and cellularity were reduced to ~ 65% of normal in $Mnt^{fl/fl}Rag1Cre$ mice, primarily due to fewer DP T cells ($P \leq 0.001$), although the DN and SP $CD4^+$ populations were also significantly reduced compared to their counterparts in $Mnt^{+/+}Rag1Cre$ controls (Fig. 1B). When the DN population was further dissected by staining with CD44 and CD25 (Supplementary Fig. S1A), it became apparent that DN4 ($CD25^-CD44^-$) cells were more affected than DN2 ($CD25^+CD44^+$) or DN3 ($CD25^+CD44^-$) cells (Fig. 1C). This deficit was not due to a failure of TCR b gene rearrangement because intracellular TCRb protein was readily detectable in the $Mnt^{fl/fl}Rag1Cre$ DN4 cells (Supplementary Fig. S1B).

Spleen cellularity was also reduced in young $Mnt^{fl/fl}Rag1Cre$ mice ($p < 0.0001$) (Fig. 1D), primarily due to the decrease in the B lymphoid population (~ 37%; $p < 0.0001$), as reported previously [15]. In addition, T cells were reduced, particularly $CD4^+$ T cells (~ 60%; $p < 0.001$). Cell surface expression analysis of CD44 and CD62L showed that the proportions of naïve, memory and effector T cells were equivalent between WT and *Mnt*-null T cells (Supplementary Fig. S1C, D). Myeloid ($Mac1^+$) cellularity was unaffected (Fig. 1D), as expected from the lack of *Rag1Cre* expression in this cell lineage.

MNT loss reduces competitive fitness.

To compare MNT-deficient versus normal lymphopoiesis, we performed competitive bone marrow reconstitution experiments. Lethally irradiated $Ly5.1^+$ mice were injected with a 50:50 mixture of $Ly5.1^+$ WT cells and test $Ly5.2^+$ $Mnt^{fl/fl}Rag1Cre$ bone marrow cells, or a 50:50 mixture of $Ly5.1^+$ WT and test $Ly5.2^+$ $Mnt^{+/+}Rag1Cre$ bone marrow cells (Fig. 2A). Analysis by flow cytometry after 12 weeks (Supplementary Fig. S2) revealed that the bone marrow cells from $Mnt^{fl/fl}Rag1Cre$ mice had competed poorly against WT cells in regenerating lymphoid populations compared to those from $Mnt^{+/+}Rag1Cre$ mice. Thymi displayed a significantly lower proportion of $Ly5.2^+$ $Mnt^{fl/fl}Rag1Cre$ (gold bars) than $Ly5.2^+$ $Mnt^{+/+}Rag1Cre$ (brown bars) cells in all major thymic subpopulations (Fig. 2B). Similarly, the spleen of reconstituted mice contained significantly fewer $Mnt^{fl/fl}Rag1Cre$ than $Mnt^{+/+}Rag1Cre$ $CD4^+$ or $CD8^+$ T cells (Fig. 2C). Comparable outcomes were noted for B lineage cells in the spleen and bone marrow (Fig. 2C, D). In contrast, as anticipated, $Ly5.2^+$ $Mnt^{+/+}Rag1Cre$ and $Ly5.2^+$ $Mnt^{fl/fl}Rag1Cre$ myeloid cells, were present in comparable numbers in the spleen and bone marrow. We conclude that MNT loss puts both T and B lymphopoiesis at a significant competitive disadvantage.

MNT loss increases T cell apoptosis.

The T cell deficit in $Mnt^{fl/fl}Rag1Cre$ mice seemed likely to reflect increased apoptosis and/or reduced MYC levels. All four major thymic sub-populations in $Mnt^{fl/fl}Rag1Cre$ mice displayed a significantly increased proportion of annexin V-positive cells compared to their WT or $Mnt^{+/+}Rag1Cre$ control counterparts (Fig. 3A, Supplementary Fig. S3) and there was a similar trend for $CD4^+$ and $CD8^+$ T cells in the spleen

(Fig. 3E). However, MNT loss did not alter the levels of endogenous MYC protein in any of these populations, as shown by flow cytometric and immunoblot analysis (Fig. 3B-D). Thus, MNT loss promoted apoptosis but did not affect MYC levels.

Enhanced apoptosis probably also explains the reduced DN4 population in *Mnt*$^{fl/fl}$*Rag1Cre* mice. When sorted DN3 and DN4 cells were cultured on OP9-DL1 cells in IL-7, conditions which are permissive for proliferation and differentiation (Fig. 4A), MYC levels and proliferation were unaffected (Supplementary Fig. S4A, B). However, the *Mnt* KO DN4 cells produced considerably fewer viable cells, of all differentiation stages, than *Mnt* WT DN4 cells (Fig. 4B, C). In contrast, the DN3 cultures showed no major differences. These observations suggest that MNT loss renders DN4 cells, but not DN3 cells, more vulnerable to apoptosis during culture.

MNT loss increased apoptosis of splenic CD4$^+$ T cells activated *in vitro* by PMA and ionomycin. The proportion of annexin-V-positive cells was ~ two-fold higher in the *Mnt* KO than the *Mnt*$^{+/+}$ CD4$^+$ T cell population and there were fewer viable cells (Fig. 4D, Supplementary Fig. S4C). In contrast, MNT loss had little consequence for CD8$^+$ T cells under these conditions.

Taken together, these observations suggest that the major determinant of the T cell deficit in *Mnt*$^{fl/fl}$*Rag1Cre* mice is increased apoptosis.

BIM is a critical mediator of apoptosis in MNT-null T cells.

Cellular stress provokes apoptosis via the mitochondrial cell death pathway, which is regulated by opposing factions of the BCL-2 family [32, 33]) and genetic studies have identified pro-apoptotic BIM (BCL2L11), a BH3-only protein, as a key trigger of lymphocyte death[34, 35, 36, 37]. We therefore hypothesised that BIM contributed to the enhanced apoptosis of MNT-deficient T cells. Notably, western blot analysis and intracellular flow cytometry revealed increased BIM protein in *Mnt* KO DP thymocytes compared to WT DP thymocytes but no significant change in pro-survival MCL-1, an important regulator of T cell survival [38] (Fig. 5A, B). Increased *Bim* transcription in MNT-deficient T cells (Fig. 5C) may at least partly account for the increased BIM protein. BIM protein was also notably higher in mitogen-activated *Mnt* KO CD4$^+$ splenic T cells, but not in mitogen-activated CD8$^+$ T cells (Fig. 4E, F), paralleling their apoptosis susceptibility under these conditions (Fig. 4D). These results suggest that MNT suppresses *Bim* expression in T lymphoid cells, as we have previously proposed for B lymphoid cells [15].

To directly test BIM involvement in the apoptosis of MNT-deficient T cells, we bred *Bim*$^{+/-}$ *Mnt*$^{fl/fl}$*Rag1Cre* mice (*Bim* is functionally haplo-insufficient [39]). Indeed, apoptosis in thymocyte populations from *Bim*$^{+/-}$ *Mnt*$^{fl/fl}$*Rag1Cre* mice (rust bars) was significantly less than in those from *Mnt*$^{fl/f}$ *Rag1Cre* mice (gold bars), and comparable to that in WT mice (black bars) (Fig. 5D). Furthermore, the cellularity of the major thymic sub-populations was restored (Fig. 5E), as was that of the DN4 sub-population (Fig. 5F). Splenic T cell cellularity was also restored to normal in the *Bim*$^{+/-}$ *Mnt*$^{fl/fl}$*Rag1Cre* mice (Fig. 5G). Furthermore, loss

of one *Bim* allele prevented the enhanced apoptosis of *Mnt*$^{fl/fl}$*Rag1Cre* CD4^{+} splenic T cells stimulated *in vitro* by PMA + ionomycin (Fig. 5H).

In summary, MNT loss upregulates BIM, thereby enhancing the vulnerability of T cells to apoptosis during normal T lymphopoiesis. Importantly, MNT may also constrain BIM levels in other cell types. We found that *MNT* KO HEK 293T cells and HeLa cells have more BIM than their parental cells, and BIM was reduced when *MNT* was reintroduced into *MNT* KO cells (Supplementary Fig. S5A-F).

Mnt **deletion prevents T lymphoma development in** MYC10^{hom} **transgenic mice.**

To ascertain the impact of MNT loss on MYC-driven T lymphomagenesis, we utilised our *MYC10*^{hom} mice [26, 40], which are homozygous for a transgene expressing a human *MYC* cDNA via the pan-haemopoietic *VavP* transgenic vector [41]. In these mice, expression of transgenic MYC protein in T lymphoid cells is significantly higher than in B lymphoid and myeloid cells, and thymic T lymphoma is the major cause of morbidity, although they also develop disseminated histiocytic myeloid (monocyte/macrophage) (Mac1^{+}F4/80^{+}Gr1^{-}) tumours affecting the spleen and other organs [40].

Mnt $^{fl/fl}$ *MYC10* ^{hom} */ Rag1Cre* mice survived significantly longer than the control *Mnt*$^{+/+}$*MYC10*^{hom} and *Mnt*$^{+/+}$*MYC10*^{hom}*/ Rag1Cre* mice (median of 158 d compared to 136 d and 148 d; $p \leq 0.001$, $p \leq 0.01$ respectively) (Fig. 6A**)** and autopsy of euthanased sick mice revealed a major difference in pathology. Whereas the control mice presented with massively enlarged thymi and/or splenomegaly, *Mnt*$^{fl/fl}$*MYC10*^{hom}*/ Rag1Cre* mice presented only with splenomegaly (Fig. 6B).

Importantly, *Rag1Cre*-mediated *Mnt* deletion had specifically prevented T lymphoma development in *MYC10*^{hom} mice (Fig. 6C). None of the 26 mice in the *Mnt*$^{fl/f}$ *MYC10*^{hom}*/Rag1Cre* cohort developed thymic T lymphomas (Supplementary Table S3) and, where analysed, their thymic T cells were polyclonal (e.g. # 1313 and #1316 in Fig. 6D). In contrast, 12/26 *Mnt*$^{+/+}$*MYC10*^{hom} and 7/24 *Mnt*$^{+/+}$*MYC10*^{hom}*/Rag1Cre* control mice developed massive thymi (up to 1440 mg) and 14/15 of those immunophenotyped were CD4^{+}CD8^{+} T lymphomas (the other being a CD19^{+} B lymphoma) **(**Supplementary Fig. S6A-C and Tables S1, S2**)**. Seven of these thymic T lymphomas analysed by PCR showed 1 or 2 dominant TCRb gene rearrangements, indicative of clonality/biclonality (Fig. 6D, E). Curiously, the T lymphomas were also Mac-1-positive (Supplementary Fig. S6A, B**)** (see Discussion).

Grossly enlarged spleens arising in either *Mnt*$^{+/+}$ or *Mnt* KO *MYC10*^{hom} mice contained a high proportion of Mac-1^{+} myeloid cells (Fig. 6F), which were transplantable (Supplementary Table S4), and histological review revealed invasion of many other tissues, as described previously [40]. However, although the splenic CD4^{+} T cells were clearly activated (CD44^{+}CD62L^{-}) (Supplementary Fig. S6D), they were not transplantable (Supplementary Table S4).

In summary, our data establish that lymphoid-specific *Mnt* deletion prevented MYC-driven T lymphomagenesis in *MYC10*^{hom} transgenic mice but not the development of fatal MYC-driven myeloid

tumours. Whether MYC-driven myeloid tumorigenesis in *vavP-MYC* transgenic mice requires MNT is not addressed by these studies as *Rag1Cre* is only expressed in lymphoid progenitor cells [42].

MNT loss impairs T cell development in MYC10^{hom} **transgenic mice.**

To clarify why T lymphomagenesis was abrogated in *Mnt$^{fl/fl}$MYC10^{hom}/Rag1Cre* mice, we analysed healthy young (8 wk-old) mice. PCR and western blot analysis of DP thymocytes confirmed efficient *Mnt* deletion (not shown**).** Of note, thymic cellularity was reduced ~ 50% in *Mnt$^{fl/fl}$MYC10^{hom}/ Rag1Cre* mice (green) compared to control *Mnt$^{+/+}$MYC10^{hom}* mice (blue) ($p \leq 0.001$), and all thymocyte sub-populations were reduced around two-fold (Fig. 7A).

As reported previously [40], the level of MYC protein in thymocytes of *MYC10^{hom}* transgenic mice greatly exceeds endogenous MYC levels (compare first 2 tracks in Fig. 7D). Concomitantly, MNT levels are also elevated 3-fold (Fig. 7D, Supplementary Fig. S7A).

MNT loss did not affect MYC protein level or cell size in premalignant *MYC10*^{hom} T cells (Supplementary Fig. S7B to D). However, as shown in Fig. 7B, the proportions of annexin-V-positive cells were significantly higher in *Mnt* KO *MYC10*^{hom} than *Mnt*$^{+/+}$ *MYC10*^{hom} thymocyte sub-populations (compare green to blue bars), which in turn tended to be higher than comparable WT sub-populations (compare blue to black bars). Furthermore, when cultured *in vitro*, *Mnt* KO *MYC10*^{hom} DP thymocytes died faster than their *Mnt*$^{+/+}$*MYC10*^{hom} or WT counterparts (Fig. 7C). Thus, the overt consequence of MNT loss was increased apoptosis.

Elevated BIM protein levels paralleled the increased apoptosis, as shown by immunoblot and intracellular FACS analysis of DP thymocytes (Fig. 7D, E), and RT PCR analysis suggested the rise at least in part reflected increased *Bim* transcription (Fig. 7F). Anti-apoptotic MCL-1 protein levels were higher in the *MYC10*^{hom} than WT DP thymocytes, but they were not affected by MNT loss (Fig. 7D). BCL-X_L levels were comparable in cells from all three genotypes (Supplementary Fig. S7A) and expression of pro-apoptotic p53 was not detectable in T cells from these healthy young *Mnt$^{fl/fl}$MYC10*^{hom} mice, by either western blot or qRT-PCR analyses (not shown).

MNT loss also resulted in a deficit of $CD4^+$ and $CD8^+$ T cells in the spleen of premalignant *MYC10*^{hom} mice (green bars in Fig. 7G). This might have been due partly to reduced migration from the thymus, but annexin V staining (Fig. 7H) indicated that they were also more susceptible to apoptosis. Pertinently, the high MYC levels did not further increase in the absence of MNT (Supplementary Fig. S8A, B). Staining for CD44 and CD62L indicated that the *MYC* trangenic splenic T cells were enlarged and highly activated, particularly the $CD4^+$ cells lacking MNT (Supplementary Fig. S8C, D).

MNT loss also greatly reduced $CD19^+$ B lymphoid cells in the spleen and bone marrow of the young *MYC10*^{hom} mice, as reported previously for pre-leukaemic *Mnt$^{fl/fl}$ Em-Myc/Rag1Cre* mice [15], but myeloid cells ($Mac1^+$, $Gr1^+$, $Mac1^+Gr1^+$) were unaffected (Fig. 7G, Supplementary Fig. S9C). Indeed, myeloid cell

numbers were still normal at this age in both *MYC10*^{hom} genotypes, despite the disseminated myeloid disease that inevitably develops as the mice age.

We conclude that the abrogation of thymic lymphoma development in *Mnt* KO *MYC10*^{hom} mice is due at least in part to the increased apoptosis of their pre-malignant T lymphoid populations, driven by elevated BIM levels.

Discussion

Impact of MNT loss on normal T cell development.

Using *Rag1Cre*-mediated deletion of *Mnt* in immature lymphoid progenitor cells in otherwise normal young mice, and competitive bone marrow reconstitution of lethally irradiated mice, we have shown that MNT-deficient lymphoid cells are more vulnerable to apoptosis during their development than those expressing MNT (ref [15], this paper). MNT loss elevated apoptosis and reduced cellularity in the thymus, bone marrow and spleen. In the T lineage, the phenotype affected all major sub-populations and was apparent as early as the DN4 pro-T cell stage, during which pre-TCR and Notch-1 signalling elevates c-MYC expression [29, 30]. In the B lineage, pre-pro-B, pro-B, pre-B and B cells were all affected [15].

The mild T cell phenotype of our *Mnt*$^{fl/fl}$ *Rag1Cre* mice differed markedly from that reported earlier for *Mnt*$^{fl/fl}$ *LckCre* mice [19], which had a more severe T cell loss, progressive inflammatory disease and a high predisposition to late T lymphoma. No tumours have developed in our *Mnt*$^{fl/fl}$ *Rag1Cre* colony, although we have not aged a large cohort. The phenotypic differences may be due to continuous (*Lck* promoter-driven) versus transient (*Rag1* promoter-driven) CRE expression. Continuous CRE exposure greatly perturbs T cell development [43], perhaps due to accumulated DNA breaks, and this phenotype may be exacerbated by concomitant loss of MNT. However, the reduced B lymphoid population may have contributed to the milder T phenotype in *Mnt*$^{fl/fl}$ *Rag1Cre* mice.

We found that MNT loss in T cells provoked upregulation of BIM, a major apoptosis trigger (e.g. [34, 35, 36, 37]), as we reported previously for B lymphoid cells [15]. Both BIM protein and *Bim* mRNA levels were elevated in T cells of *Mnt*$^{fl/fl}$ *Rag1Cre* mice. Importantly, the enhanced apoptosis and T cell deficit provoked by lymphoid-specific *Mnt* KO was reversed by loss of a single *Bim* allele. MNT may directly suppress *Bim* transcription, as MNT binding sites in the *Bim* locus have been identified in mouse B cells (see CUT&RUN data GSE132967 reported by Mathsyaraja et al [44]). Importantly, our data with human HEK 293T and HeLa cells (Supplementary Fig. S5) suggest that MNT can also dampen BIM expression in non-lymphoid cell types. Indirect as well as direct mechanisms may be involved.

Impact of MNT loss on T lymphomagenesis.

To gauge how MNT affects MYC-driven T lymphomagenesis, we utilised VavP-*MYC10*^{hom} mice, in which transgene expression is pan-haemopoietic but highest in T cells [26, 40]. These mice are prone to both

thymic T lymphomas and disseminated myeloid tumours. Strikingly, lymphoid-specific *Mnt* loss totally ablated T lymphoma development in the *MYC10*^{hom} mice. *None* of the mice in the *Mnt*$^{fl/fl}$*MYC10*^{hom}*/Rag1Cre* cohort (n = 26) developed thymic lymphomas. Instead, their morbidity was exclusively due to highly invasive myeloid tumour cells.

In contrast, approximately 40% of the 50 control *Mnt* WT *MYC* transgenic mice (*Mnt*$^{+/+}$*MYC10*^{hom} plus *Mnt*$^{+/+}$*MYC10*^{hom}*/Rag1Cre*) developed thymic lymphomas. Apart from one CD19^{+} lymphoma, all 15 thymic tumours immunophenotyped in these mice were unusual CD4^{+}CD8^{+} T lymphomas expressing Mac-1. Activated CD8^{+} T cells express Mac-1[45], so its expression on the DP T lymphomas may reflect activation induced by the *MYC10*^{hom} transgene. Alternatively, these tumours may arise from a T/myeloid progenitor cell, as do rare mixed-phenotype human acute leukaemias (e.g. ref [46, 47]).

Our results showing that MNT loss abrogates T lymphomagenesis confirm and extend those reported by Hurlin's group for transgenic mice engineered for T cell-specific (*Lck-Cre*-dependent) expression of a stable mutant MYC^{T58A} protein from within the ROSA 26 locus [20, 48].

To explore why T lymphomas failed to develop in *Mnt* KO *MYC10*^{hom} mice, we compared phenotypes of young mice, prior to any sign of emerging malignancy. MNT loss halved T cell numbers in both the thymus and spleen, and the *Mnt* KO *MYC10*^{hom} T cells were significantly more susceptible to apoptosis than *Mnt*$^{+/+}$*MYC10*^{hom} T cells, at all major stages of development. Indeed, their apoptosis is likely to be much greater than suggested by annexin-V labelling, as apoptotic cells are very rapidly engulfed by phagocytes *in vivo* [49].

Quantification of the expression of major apoptosis regulators revealed that pro-apoptotic BIM was elevated in *Mnt* KO as compared to *Mnt*$^{+/+}$ DP thymocytes in *MYC10*^{hom} transgenic mice. In contrast, the transcription factor TP53, which triggers apoptosis by transcriptionally activating expression of two other pro-apoptotic BH3-only proteins, PUMA and NOXA, was undetectable. Moreover, the level of MCL-1, an important regulator of T cell survival [38], was unchanged. We infer that BIM upregulation is a major factor responsible for reducing T cell populations in healthy young *Mnt* KO *MYC10*^{hom} mice.

Tumour development requires acquisition of oncogenic mutations and overcoming the protective apoptosis threshold. BIM-directed apoptosis has been shown to be one of the major factors limiting MYC-driven cellular proliferation, as loss of even one *Bim* allele greatly accelerated lymphomagenesis in Em-*Myc* mice [39]. By suppressing BIM, MNT reduces the risk of apoptosis in proliferating cells driven by MYC, thereby boosting the population at risk of acquiring oncogenic mutations. Conversely, MNT loss elevates apoptosis risk and reduces lymphoma risk.

As a MYC antagonist, MNT was originally considered a tumour suppressor and this was supported by an early study showing that mice with mammary-specific *Mnt* deletion developed mammary adenocarcinoma [22]. The tumour suppressor role received further support when focal deletions involving

the *MNT* locus (usually monoallelic) were noted in ~ 10% of cancers in The Human Cancer Genome Atlas [4], including certain cases of chronic lymphocytic leukaemia [24], a B cell malignancy, and Sezary syndrome, a cutaneous T-cell lymphoma/leukaemia [23]. However, *MNT* is localised on human chromosome 17p13.3 [12], near the potent tumour suppressor gene *TP53* (17p13.1), making it difficult to ascribe any impact of large deletions solely, if at all, to MNT deletion.

While MNT might act as a tumour suppressor in certain settings, genetic studies from ourselves and others (ref[15, 20, 21] and this paper), using three independent transgenic mouse models, demonstrate unequivocally that MNT *facilitates* MYC-driven lymphomagenesis, rather than acting as a tumour suppressor, and that it does so by limiting apoptosis. Importantly, we have shown that MNT suppresses apoptosis by dampening expression of BIM, one of the most important apoptosis triggers for B and T lymphoid cells [50]. Like MYC, MNT binds to E boxes near many genes [1, 44]. Therefore, in addition to suppressing apoptosis, MNT may prove to have other roles in facilitating MYC-driven oncogenesis.

MYC is a major driver for many (perhaps most) lymphoid and myeloid tumours and indeed a variety of solid tumours [3, 4]. However, the protracted search for a clinically effective MYC inhibitor has not yet succeeded [51, 52]. The realisation that MNT suppresses MYC-driven apoptosis opens an entirely new therapeutic approach: inhibition of MNT to amplify MYC's capacity to drive apoptosis.

Declarations

ACKNOWLEDGEMENTS

The authors thank Peter Hurlin (Shriner's Hospital for Children, Portland OR USA) for his kind gift of *Mnt* floxed mice; our colleagues Jerry Adams, Andreas Strasser, Gemma Kelly, Steve Nutt and Jacob Jackson for comments on the manuscript and useful discussions; Steve Nutt and Andreas Strasser and Lorraine O'Reilly for fluorescent antibodies; Krystal Hughes, Crystal Stivala, Michael Watters, Sam Kelly, Dan Fayle and Giovanni Siciliano for mouse husbandry; Simon Monard for assistance with flow cytometry; and Peter Maltezos for skilful preparation of Figures.

AUTHOR CONTRIBUTIONS

H.V.N, C.J.V and M.R.R. performed the experiments; A.P.N performed histological analysis; S.C. conceived the project, wrote the manuscript with input from the authors and secured funding.

FUNDING

This work was supported by grants from the National Health and Medical Research Council (NHMRC) (program grant 1016701), the Leukemia & Lymphoma Society (SCOR grant 7001-13) and a Grant-in-Aid from the Cancer Council Victoria App 118768 (to SC); NHMRC project grants GNT1060179 and GNT1122783 (to APN), philanthropic support to the Walter and Eliza Hall Institute; and operational infrastructure grants through the Australian Government IRISS and the Victorian Government OIS.

COMPETING INTERESTS

The authors declare no competing financial interests.

ADDITIONAL INFORMATION

Supplementary information The online version contains supplementary material available at

Correspondence: Suzanne Cory, The Walter and Eliza Hall Institute of Medical Research, 1G Royal Parade, VIC 3052, Australia; e-mail: cory@wehi.edu.au.

References

1. Diolaiti D, McFerrin L, Carroll PA, Eisenman RN. Functional interactions among members of the MAX and MLX transcriptional network during oncogenesis. Biochim Biophys Acta 2015, **1849**(5): 484–500.
2. Kress TR, Sabo A, Amati B. MYC: connecting selective transcriptional control to global RNA production. Nat Rev Cancer 2015, **15**(10): 593–607.
3. Kalkat M, De Melo J, Hickman KA, Lourenco C, Redel C, Resetca D, *et al.* MYC Deregulation in Primary Human Cancers. Genes (Basel) 2017, **8**(6).
4. Schaub FX, Dhankani V, Berger AC, Trivedi M, Richardson AB, Shaw R, *et al.* Pan-cancer Alterations of the MYC Oncogene and Its Proximal Network across the Cancer Genome Atlas. Cell Syst 2018, **6**(3): 282–300 e282.
5. Askew DS, Ashmun RA, Simmons BC, Cleveland JL. Constitutive c-*myc* expression in an IL-3-dependent myeloid cell line suppresses cell cycle arrest and accelerates apoptosis. Oncogene 1991, **6**: 1915–1922.
6. Evan GI, Wyllie AH, Gilbert CS, Littlewood TD, Land H, Brooks M, *et al.* Induction of apoptosis in fibroblasts by c-myc protein. Cell 1992, **69**: 119–128.
7. Murphy DJ, Junttila MR, Pouyet L, Karnezis A, Shchors K, Bui DA, *et al.* Distinct thresholds govern Myc's biological output in vivo. Cancer Cell 2008, **14**(6): 447–457.
8. Vaux DL, Cory S, Adams JM. *Bcl*-2 gene promotes haemopoietic cell survival and cooperates with c-*myc* to immortalize pre-B cells. Nature 1988, **335**: 440–442.
9. Strasser A, Harris AW, Bath ML, Cory S. Novel primitive lymphoid tumours induced in transgenic mice by cooperation between *myc* and *bcl*-2. Nature 1990, **348**(6299): 331–333.
10. Grandori C, Cowley SM, James LP, Eisenman RN. The Myc/Max/Mad network and the transcriptional control of cell behavior. Annu Rev Cell Dev Biol 2000, **16**: 653–699.
11. Hurlin PJ, Queva C, Eisenman RN. Mnt, a novel Max-interacting protein is coexpressed with Myc in proliferating cells and mediates repression at Myc binding sites. Genes Dev 1997, **11**(1): 44–58.
12. Meroni G, Reymond A, Alcalay M, Borsani G, Tanigami A, Tonlorenzi R, *et al.* Rox, a novel bHLHZip protein expressed in quiescent cells that heterodimerizes with Max, binds a non-canonical E box and

acts as a transcriptional repressor. EMBO J 1997, **16**(10): 2892–2906.

13. Liano-Pons J, Arsenian-Henriksson M, Leon J. The Multiple Faces of MNT and Its Role as a MYC Modulator. Cancers (Basel) 2021, **13**(18).
14. Toyo-oka K, Hirotsune S, Gambello MJ, Zhou ZQ, Olson L, Rosenfeld MG, *et al.* Loss of the Max-interacting protein Mnt in mice results in decreased viability, defective embryonic growth and craniofacial defects: relevance to Miller-Dieker syndrome. Hum Mol Genet 2004, **13**(10): 1057–1067.
15. Nguyen HV, Vandenberg CJ, Ng AP, Robati MR, Anstee NS, Rimes J, *et al.* Development and survival of MYC-driven lymphomas require the MYC antagonist MNT to curb MYC-induced apoptosis. Blood 2020, **135**(13): 1019–1031.
16. Adams JM, Harris AW, Pinkert CA, Corcoran LM, Alexander WS, Cory S, *et al.* The c-myc oncogene driven by immunoglobulin enhancers induces lymphoid malignancy in transgenic mice. Nature 1985, **318**(6046): 533–538.
17. Vose J, Armitage J, Weisenburger D. International peripheral T-cell and natural killer/T-cell lymphoma study: pathology findings and clinical outcomes. J Clin Oncol 2008, **26**(25): 4124–4130.
18. Horwitz S, O'Connor OA, Pro B, Illidge T, Fanale M, Advani R, *et al.* Brentuximab vedotin with chemotherapy for CD30-positive peripheral T-cell lymphoma (ECHELON-2): a global, double-blind, randomised, phase 3 trial. Lancet 2019, **393**(10168): 229–240.
19. Dezfouli S, Bakke A, Huang J, Wynshaw-Boris A, Hurlin PJ. Inflammatory disease and lymphomagenesis caused by deletion of the Myc antagonist Mnt in T cells. Mol Cell Biol 2006, **26**(6): 2080–2092.
20. Link JM, Ota S, Zhou ZQ, Daniel CJ, Sears RC, Hurlin PJ. A critical role for Mnt in Myc-driven T-cell proliferation and oncogenesis. Proc Natl Acad Sci U S A 2012, **109**(48): 19685–19690.
21. Campbell KJ, Vandenberg CJ, Anstee NS, Hurlin PJ, Cory S. Mnt modulates Myc-driven lymphomagenesis. Cell Death Differ 2017, **24**(12): 2117–2126.
22. Toyo-oka K, Bowen TJ, Hirotsune S, Li Z, Jain S, Ota S, *et al.* Mnt-deficient mammary glands exhibit impaired involution and tumors with characteristics of myc overexpression. Cancer Res 2006, **66**(11): 5565–5573.
23. Vermeer MH, van Doorn R, Dijkman R, Mao X, Whittaker S, van Voorst Vader PC, *et al.* Novel and highly recurrent chromosomal alterations in Sezary syndrome. Cancer Res 2008, **68**(8): 2689–2698.
24. Edelmann J, Holzmann K, Miller F, Winkler D, Buhler A, Zenz T, *et al.* High-resolution genomic profiling of chronic lymphocytic leukemia reveals new recurrent genomic alterations. Blood 2012, **120**(24): 4783–4794.
25. McCormack MP, Forster A, Drynan L, Pannell R, Rabbitts TH. The LMO2 T-cell oncogene is activated via chromosomal translocations or retroviral insertion during gene therapy but has no mandatory role in normal T-cell development. Mol Cell Biol 2003, **23**(24): 9003–9013.
26. Smith DP, Bath ML, Harris AW, Cory S. T-cell lymphomas mask slower developing B-lymphoid and myeloid tumors in transgenic mice with broad hematopoietic expression of MYC. Oncogene 2005, **24**(22): 3544–3553.

27. Bouillet P, Cory S, Zhang L-C, Strasser A, Adams JM. Degenerative disorders caused by Bcl-2 deficiency are prevented by loss of its BH3-only antagonist Bim. Dev Cell 2001, **1**(5): 645–653.
28. Schmitt TM, Zúñiga-Pflücker JC. Induction of T cell development from hematopoietic progenitor cells by Delta-like-1 in vitro. Immunity 2002, **17**(6): 749–756.
29. Douglas NC, Jacobs H, Bothwell AL, Hayday AC. Defining the specific physiological requirements for c-Myc in T cell development. Nat Immunol 2001, **2**(4): 307–315.
30. Dose M, Khan I, Guo Z, Kovalovsky D, Krueger A, von Boehmer H, *et al.* c-Myc mediates pre-TCR-induced proliferation but not developmental progression. Blood 2006, **108**(8): 2669–2677.
31. Nozais M, Loosveld M, Pankaew S, Grosjean C, Gentil N, Quessada J, *et al.* MYC deficiency impairs the development of effector/memory T lymphocytes. iScience 2021, **24**(7): 102761.
32. Strasser A, Cory S, Adams JM. Deciphering the rules of programmed cell death to improve therapy of cancer and other diseases. EMBO J 2011, **30**(18): 3667–3683.
33. Czabotar PE, Lessene G, Strasser A, Adams JM. Control of apoptosis by the BCL-2 protein family: implications for physiology and therapy. Nat Rev Mol Cell Biol 2014, **15**(1): 49–63.
34. Bouillet P, Metcalf D, Huang DCS, Tarlinton DM, Kay TWH, Köntgen F, *et al.* Proapoptotic Bcl-2 relative Bim required for certain apoptotic responses, leukocyte homeostasis, and to preclude autoimmunity. Science 1999, **286**(5445): 1735–1738.
35. Bouillet P, Purton JF, Godfrey DI, Zhang L-C, Coultas L, Puthalakath H, *et al.* BH3-only Bcl-2 family member Bim is required for apoptosis of autoreactive thymocytes. Nature 2002, **415**: 922–926.
36. Hildeman DA, Zhu Y, Mitchell TC, Bouillet P, Strasser A, Kappler J, *et al.* Activated T cell death in vivo mediated by pro-apoptotic Bcl-2 family member, Bim. Immunity 2002, **16**: 759–767.
37. Pellegrini M, Bouillet P, Robati M, Belz GT, Davey GM, Strasser A. Loss of Bim Increases T Cell Production and Function in Interleukin 7 Receptor-deficient Mice. J Exp Med 2004, **200**(9): 1189–1195.
38. Opferman JT, Letai A, Beard C, Sorcinelli MD, Ong CC, Korsmeyer SJ. Development and maintenance of B and T lymphocytes requires antiapoptotic MCL-1. Nature 2003, **426**(6967): 671–676.
39. Egle A, Harris AW, Bouillet P, Cory S. Bim is a suppressor of Myc-induced mouse B cell leukemia. Proc Natl Acad Sci U S A 2004, **101**(16): 6164–6169.
40. Smith DP, Bath ML, Metcalf D, Harris AW, Cory S. MYC levels govern hematopoietic tumor type and latency in transgenic mice. Blood 2006, **108**(2): 653–661.
41. Ogilvy S, Metcalf D, Gibson L, Bath ML, Harris AW, Adams JM. Promoter elements of *vav* drive transgene expression *in vivo* throughout the hematopoietic compartment. Blood 1999, **94**(6): 1855–1863.
42. Kuo TC, Schlissel MS. Mechanisms controlling expression of the RAG locus during lymphocyte development. Curr Opin Immunol 2009, **21**(2): 173–178.
43. Carow B, Gao Y, Coquet J, Reilly M, Rottenberg ME. lck-Driven Cre Expression Alters T Cell Development in the Thymus and the Frequencies and Functions of Peripheral T Cell Subsets. J

Immunol 2016, **197**(6): 2261–2268.

44. Mathsyaraja H, Freie B, Cheng PF, Babaeva E, Catchpole JT, Janssens D, *et al.* Max deletion destabilizes MYC protein and abrogates Emicro-Myc lymphomagenesis. Genes Dev 2019, **33**(17–18): 1252–1264.
45. Christensen JE, Andreasen SO, Christensen JP, Thomsen AR. CD11b expression as a marker to distinguish between recently activated effector CD8(+) T cells and memory cells. International Immunology 2001, **13**(4): 593–600.
46. Alexander TB, Gu Z, Iacobucci I, Dickerson K, Choi JK, Xu B, *et al.* The genetic basis and cell of origin of mixed phenotype acute leukaemia. Nature 2018, **562**(7727): 373–379.
47. Fishman H, Madiwale S, Geron I, Bari V, Van Loocke W, Kirschenbaum Y, *et al.* ETV6-NCOA2 fusion induces T/Myeloid mixed-phenotype leukemia by transformation of non-thymic hematopoietic progenitors. *Blood* 2022.
48. Wang X, Cunningham M, Zhang X, Tokarz S, Laraway B, Troxell M, *et al.* Phosphorylation regulates c-Myc's oncogenic activity in the mammary gland. Cancer Res 2011, **71**(3): 925–936.
49. Dzhagalov IL, Chen KG, Herzmark P, Robey EA. Elimination of self-reactive T cells in the thymus: a timeline for negative selection. PLoS Biol 2013, **11**(5): e1001566.
50. Strasser A, Bouillet P. The control of apoptosis in lymphocyte selection. Immunol Rev 2003, **193**: 82–92.
51. Dang CV, Reddy EP, Shokat KM, Soucek L. Drugging the 'undruggable' cancer targets. Nat Rev Cancer 2017, **17**(8): 502–508.
52. Chen H, Liu H, Qing G. Targeting oncogenic Myc as a strategy for cancer treatment. Signal Transduct Target Ther 2018, **3**: 5.
53. Mingueneau M, Kreslavsky T, Gray D, Heng T, Cruse R, Ericson J, *et al.* The transcriptional landscape of alphabeta T cell differentiation. Nat Immunol 2013, **14**(6): 619–632.

Figures

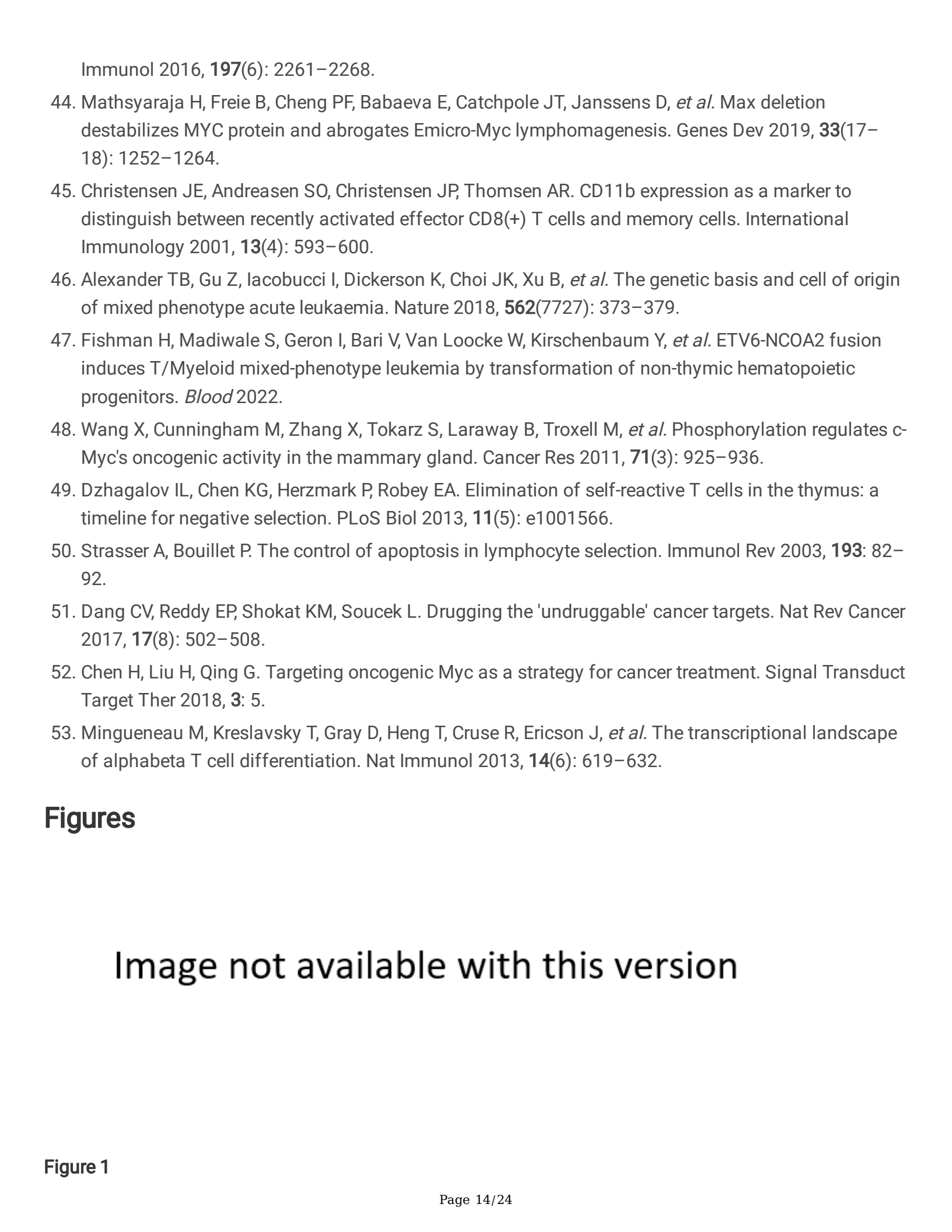

Figure 1

MNT loss impairs normal T cell development. (A) *Mnt* deletion mediated by *Rag1Cre* gene is highly efficacious. Typical PCR (left) and western blot (right) analysis of indicated T cell sub-populations sorted from thymi of 6-7 wk-old WT and $Mnt^{fl/fl}$ *Rag1Cre* (KO) mice. In left panel, * indicates primer dimer. (B) $Mnt^{fl/fl}$ *Rag1Cre* mice exhibit modest T cell deficit. (L to R) Weight, cellularity and flow cytometric quantification of DN, DP, SP CD4+ and SP $CD8^+$ T cells in thymi of 6-7 wk-old mice of indicated genotypes. (C) DN sub-population analysis (see Supplementary Fig. 1) reveals significant reduction of DN4 ($CD4^-CD8^-CD25^-CD44^-$) cells in $Mnt^{fl/fl}$ *Rag1Cre* mice. (D) Splenic T and B cells, but not myeloid cells, are reduced in $Mnt^{fl/fl}$ *Rag1Cre* mice. Cell preparations from thymi and spleens of 6-7 wk-old mice were analysed by flow cytometry (n = 4 to 21); genotypes shown are WT (black), $Mnt^{+/+}$*Rag1Cre* (brown) and $Mnt^{fl/fl}$*Rag1Cre* (gold); dots indicate individual mice, bars show mean SEM; * P£ 0.05, ** P £ 0.01; *** P £ 0.001; **** P £ 0.0001, ns=not significant.

Image not available with this version

Figure 2

Bone marrow reconstitution reveals competitive disadvantage of MNT-null lymphopoiesis. (A) Protocol for competitive reconstitution. C57BL/6 mice ($Ly5.1^+$) (3-4 per test) were lethally irradiated (2 x 550 Rad) and injected with a 1:1 mixture of bone marrow cells (10^6 cells per genotype) from $Ly5.1^+$ C57BL/6 mice (competitor cells) and either $Mnt^{+/+}$*Rag1Cre* or $Mnt^{fl/fl}$*Rag1Cre* mice ($Ly5.2^+$ test cells). (B, C, D) Relative proportions of reconstituted test cells ($Ly5.2^+$) and competitor cells ($Ly5.1^+$) of the indicated cell types in the thymus (B), spleen (C) and bone marrow (D), 12 weeks post-transplantation. Analysis was performed by flow cytometry (see Supplementary Fig. S2). Data shown are from four independent reconstitution experiments; genotypes are WT ($Ly5.1^+$, black), $Mnt^{+/+}$*Rag1Cre* ($Ly5.2^+$, brown) and $Mnt^{fl/fl}$*Rag1Cre* ($Ly5.2^+$, gold). Dots indicate individual mice, bars show mean SEM; statistical significance is shown only for $Mnt^{+/+}$*Rag1Cre* versus $Mnt^{fl/fl}$*Rag1Cre* cells; **** P £ 0.0001, ns=not significant.

Figure 3

MNT loss enhances T cell apoptosis but does not alter MYC level. (A) MNT loss increases apoptosis in all major thymic T cell sub-populations. (B-D) MNT loss does not alter MYC levels in thymic T cell sub-populations. (B) Typical intracellular MYC staining. Thymocytes were stained with CD4 and CD8 antibodies and then fixed, permeabilised and stained with MYC antibody (pink) or isotype-matched control antibody (blue). (C) Mean fluorescence intensity (MFI) for intracellular MYC ± SEM for indicated thymocyte sub-populations. (D) Typical western blot showing MNT, MYC and ACTIN protein levels in indicated thymocyte sub-populations. Note the lower MYC in DP cells, a well-documented feature of this predominantly quiescent population [53]. (E) MNT loss has minor impact on apoptosis of splenic $CD4^+$ and $CD8^+$ T cells. Apoptosis was quantified by flow cytometry after staining cells with AnnexinV-FITC. Genotypes analysed were WT (black), *Mnt*$^{+/+}$*Rag1Cre* (brown) and *Mnt*$^{fl/fl}$*Rag1Cre* (gold). Dots indicate individual mice, and bars show mean SEM; ** P £ 0.01; *** P £ 0.001; ****P £ 0.0001; ns=not significant.

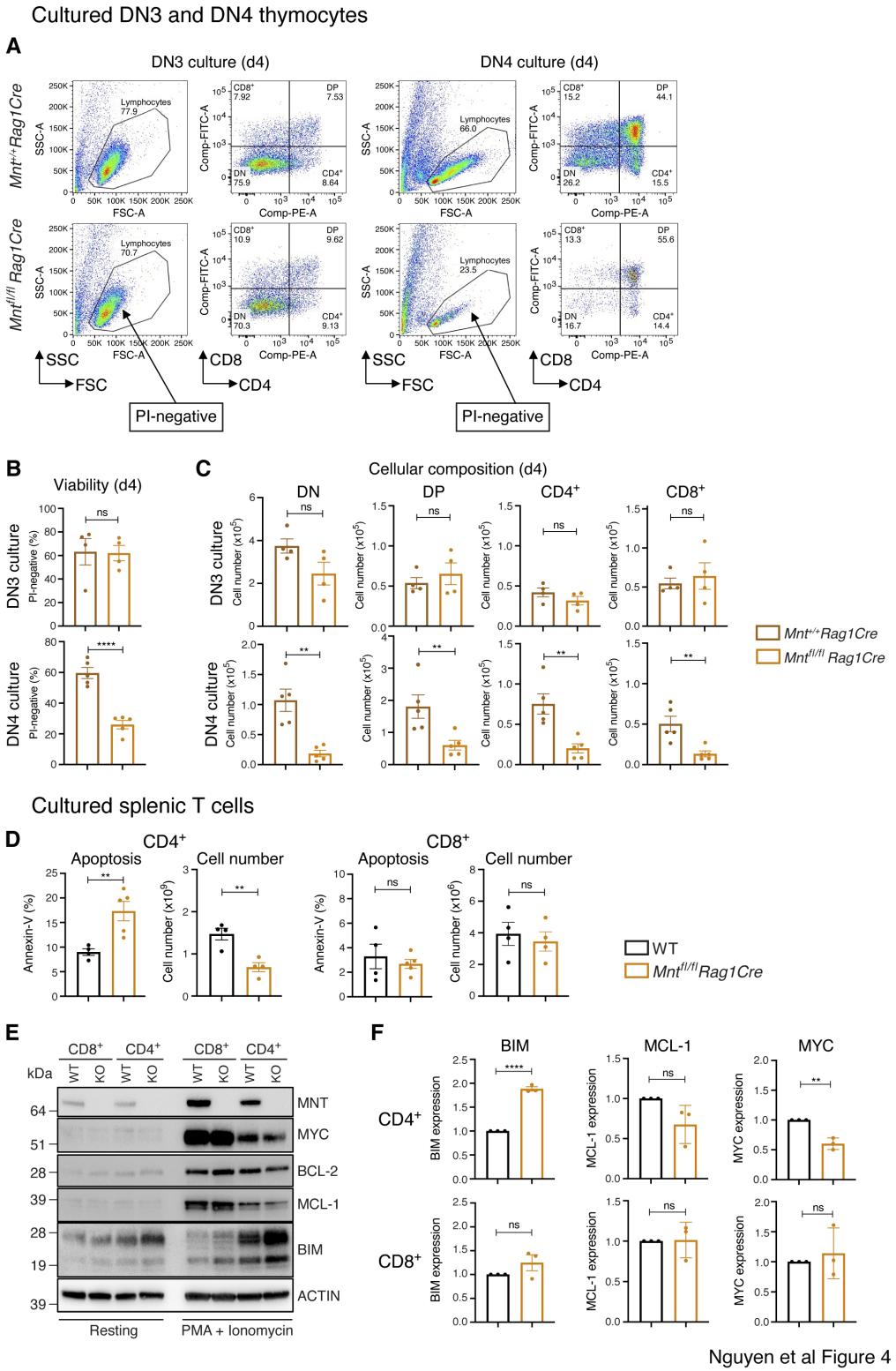

Figure 4

MNT loss increases apoptosis of thymic DN4 and splenic CD4$^+$ cells *in vitro*. (A-C) MNT loss enhances vulnerability of DN4 but not DN3 progenitor T cells to apoptosis *in vitro*. DN3 and DN4 cells sorted by FACS from thymi of *Mnt$^{fl/fl}$Rag1Cre* (gold) and control *Mnt$^{+/+}$Rag1Cre* (brown) mice were cultured in IL-7 on OP9-DL1 stromal cells and (A) analysed on d4 by flow cytometry for (B) viability and (C) differentiation. (D-F) MNT loss enhances apoptosis of stimulated CD4$^+$ but not CD8$^+$ splenic T cells.

$CD4^+$ and $CD8^+$ T cells sorted from WT and *Mnt*$^{fl/fl}$*Rag1Cre* spleens were cultured in 2mL medium containing 20 ng/mL PMA and 1mg/mL ionomycin for 72h and then analysed by flow cytometry and immunoblot. (D) Annexin V-staining (left panels) and viable cell number (right panels). (E) Typical western blot of MNT, MYC, BCL-2, MCL-1 and BIM protein before and after stimulation, with ACTIN serving as a loading control. (F) Quantification of BIM, MCL-1 and MYC protein in 3 western blots, relative to ACTIN in same blot, after stimulation; values for *Mnt*$^{fl/fl}$*Rag1Cre* cells (gold) were normalized to those for WT cells (black). Dots indicate individual mice, and bars show mean SEM; * P£ 0.05, ** P £ 0.01, **** P £ 0.0001; ns=not significant.

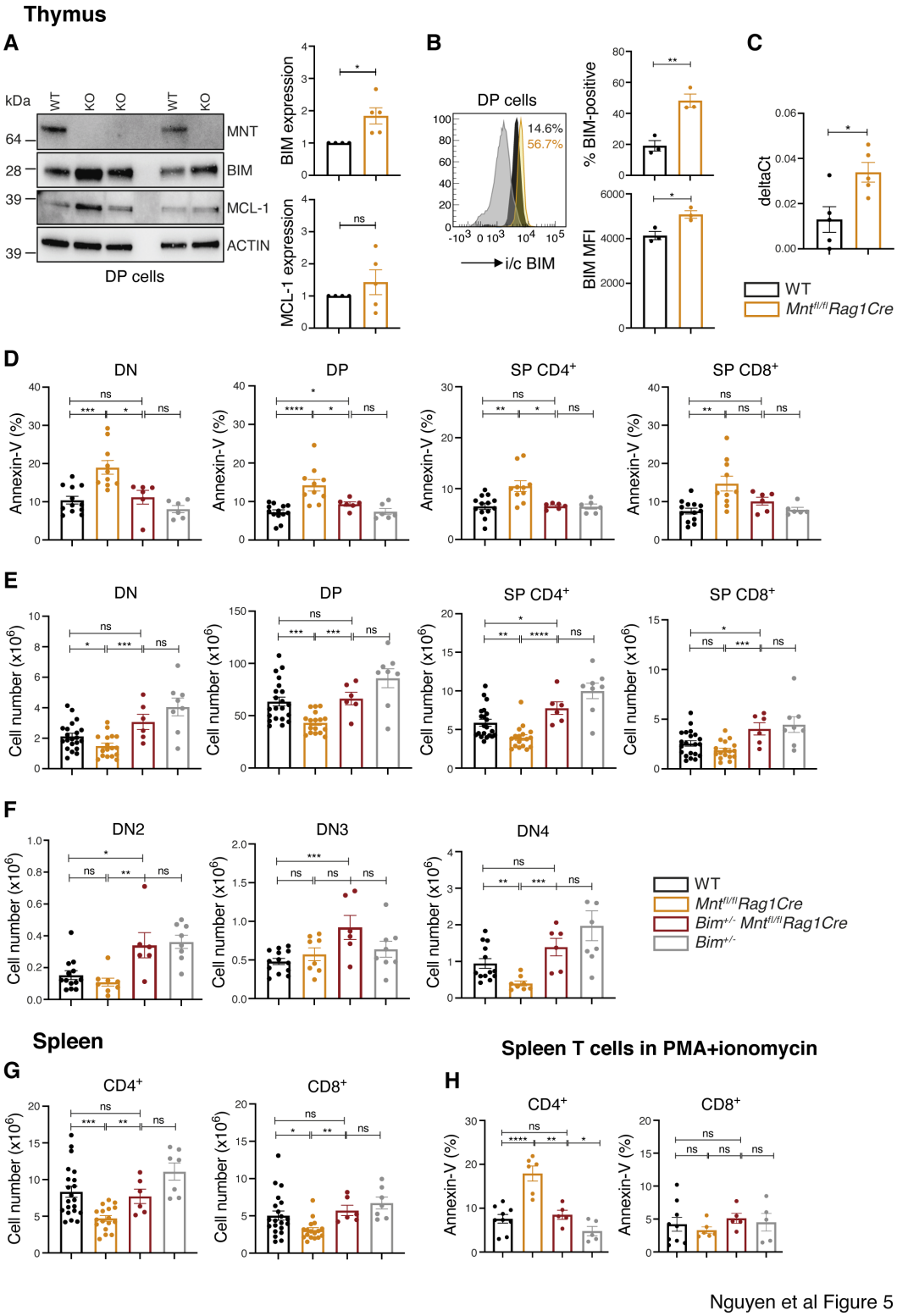

Nguyen et al Figure 5

Figure 5

Elevated BIM promotes apoptosis in *Mnt* KO T cells. (A, B) BIM protein is elevated in *Mnt* KO DP thymocytes. DP T cells were sorted from thymi of 3 independent WT and 5 independent *Mnt*$^{fl/fl}$ *Rag1Cre* mice and BIM levels quantified by immunoblot and intracellular staining. (A) Left panel shows one of two western blots and right panel quantifies BIM and MCL-1 levels for both blots relative to ACTIN and normalised to that in WT cells. (B) Left panel shows a typical FACS profile, comparing BIM level in DP

thymocytes from *Mnt*$^{fl/fl}$*Rag1Cre* (gold), WT (black) and, as a negative control, *Bim*$^{-/-}$ mice (grey). Right panels show % BIM-positive cells and Mean Fluorescence Intensity (MFI) for BIM in three independent experiments SEM. (C) *Bim* transcription is elevated in *Mnt* KO DP thymocytes. Quantitative RT-PCR of *Bim* transcripts in *Mnt*$^{fl/fl}$ *Rag1Cre* (gold) compared to WT (black) DP thymocytes; values were calculated relative to *Gapdh* control. (D) *Bim* heterozygosity ameliorates apoptosis of major T cell sub-populations in thymus of *Mnt*$^{fl/fl}$*Rag1Cre* mice. (E) *Bim* heterozygosity restores cellularity of major T cell sub-populations in thymus of *Mnt*$^{fl/fl}$*Rag1Cre* mice. (F) *Bim* heterozygosity increases the cellularity of DN2, DN3 and DN4 progenitor cell populations in thymus of *Mnt*$^{fl/fl}$*Rag1Cre* mice. (G) *Bim* heterozygosity increases CD4^{+} and CD8^{+} T cells in the spleen of *Mnt*$^{fl/fl}$ *Rag1Cre* mice. (H) *Bim* heterozygosity prevents increased apoptosis in activated CD4^{+} and CD8^{+} splenic T cells caused by MNT loss. Splenic CD4^{+} and CD8^{+} T cells from mice of the indicated genotypes were cultured in PMA + ionomycin for 72 h. Apoptosis was quantified by flow cytometry after staining cells with Annexin-V-FITC. Genotypes analysed were WT (black), *Mnt*$^{fl/fl}$*Rag1Cre* (gold), *Bim*$^{+/-}$*Mnt*$^{fl/fl}$ *Rag1Cre* (rust) and *Bim*$^{+/-}$ (grey). Dots indicate individual mice, and bars show mean SEM; * P£ 0.05, ** P £ 0.01; *** P £ 0.001; **** P £ 0.0001; ns=not significant. Data include mice in Fig. 1 plus additional mice.

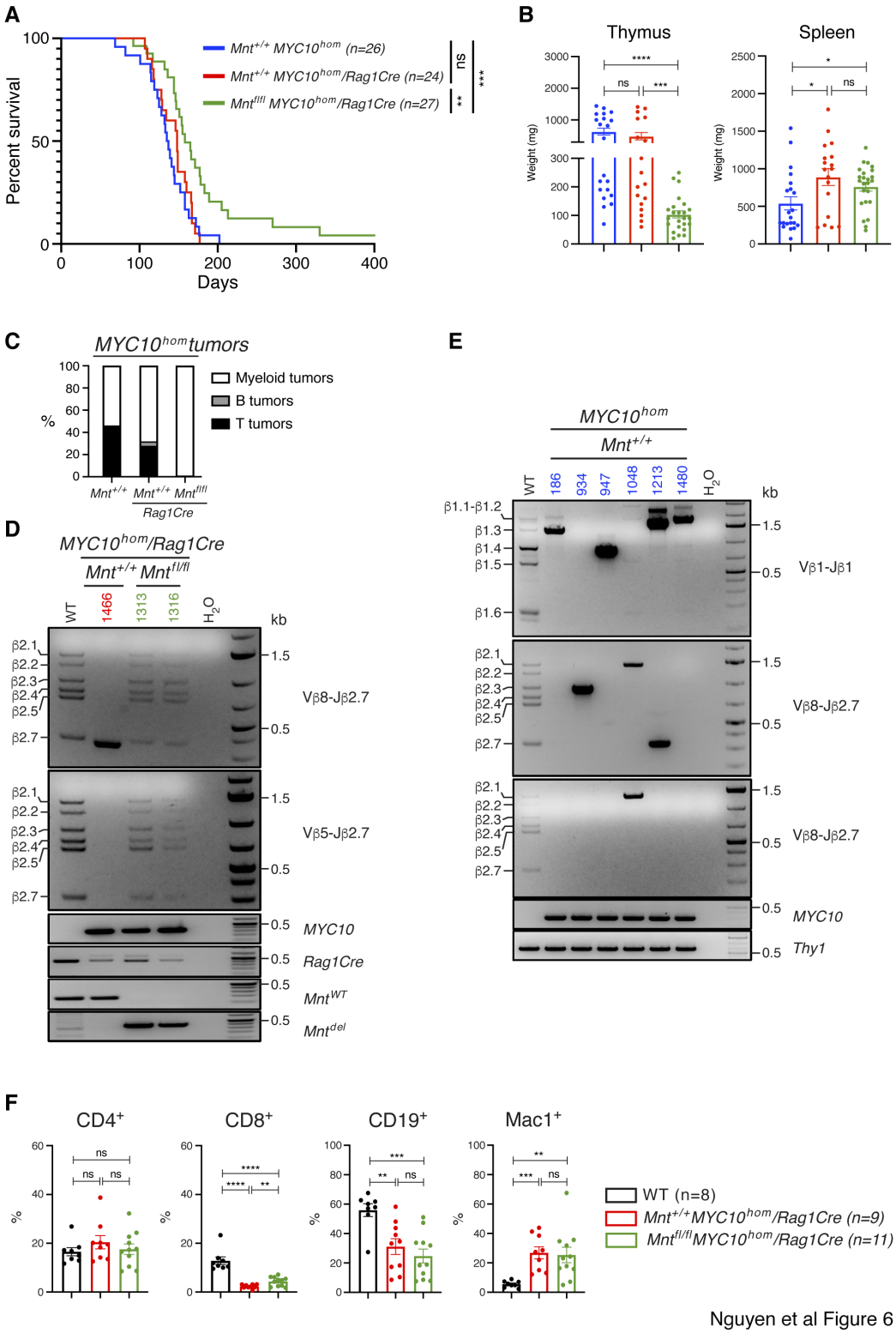

Nguyen et al Figure 6

Figure 6

Lymphoid-specific MNT loss prevents thymic lymphoma development in *Mnt$^{fl/fl}$MYC10^{hom}/Rag1Cre* mice. (A) Kaplan-Meier survival curves showing significantly delayed morbidity for *Mnt$^{fl/fl}$MYC10^{hom}/Rag1Cre* mice (green curve; median survival 162 d) compared to control *Mnt$^{+/+}$MYC10^{hom}* (blue curve; median survival 134 d) and *Mnt$^{+/+}$MYC10^{hom}/Rag1Cre* (red curve; median survival 126 d) mice. (B) MNT loss prevents thymus but not spleen enlargement. Morbid mice were

euthanased and the weights of spleens and thymi measured. Bars show mean thymus and spleen weights SEM, and dots indicate values for individual euthanased mice. (C) MNT loss prevents T lymphoma development. Proportion of T (black) and B (grey) thymic lymphomas and myeloid tumours (white) in euthanased *Mnt*$^{+/+}$*MYC10*^{hom}, *Mnt*$^{+/+}$*MYC10*^{hom}*/Rag1Cre* and *Mnt*$^{fl/fl}$*MYC10*^{hom}*/Rag1Cre* mice. (See text and Tables 1-3). (D) Polyclonality of thymic T cells in *Mnt*$^{fl/fl}$*MYC10*^{hom}*/Rag1Cre* mice. PCR analysis of *TCRb* gene rearrangements was performed on DNA isolated from DP thymic cells from *Mnt*$^{fl/fl}$*MYC10*^{hom}*/Rag1Cre* mice # 1313, #1316 (green) and, as a control, a clonal T lymphoma *Mnt*$^{+/+}$*MYC10*$^{hom/}$*Rag1Cre* mouse #1466 (red). Lower 4 panels show PCR genotype analysis. (E) Clonality of thymic T lymphomas from *Mnt*$^{+/+}$*MYC10*^{hom} mice. DNA was isolated from individual T lymphomas (blue) and genomic PCR analysis performed for indicated *TCRb* gene rearrangements, *MYC10* transgene and, as a loading control, *Thy1*. (F) Enlarged spleens from both *Mnt*$^{+/+}$ and *Mnt*$^{fl/fl}$ *MYC10*^{hom}*/Rag1Cre* mice have elevated proportion of Mac1^{+} myeloid cells. Mouse genotypes analysed were WT (black), *Mnt*$^{+/+}$*MYC10*^{hom}*/Rag1Cre* (red) and *Mnt*$^{fl/fl}$*MYC10*^{hom}*/Rag1Cre* mice (green). Dots indicate individual mice, and bars show mean % cellularity SEM; * P£ 0.05, ** P £ 0.01; *** P £ 0.001; **** P £ 0.0001; ns=not significant.

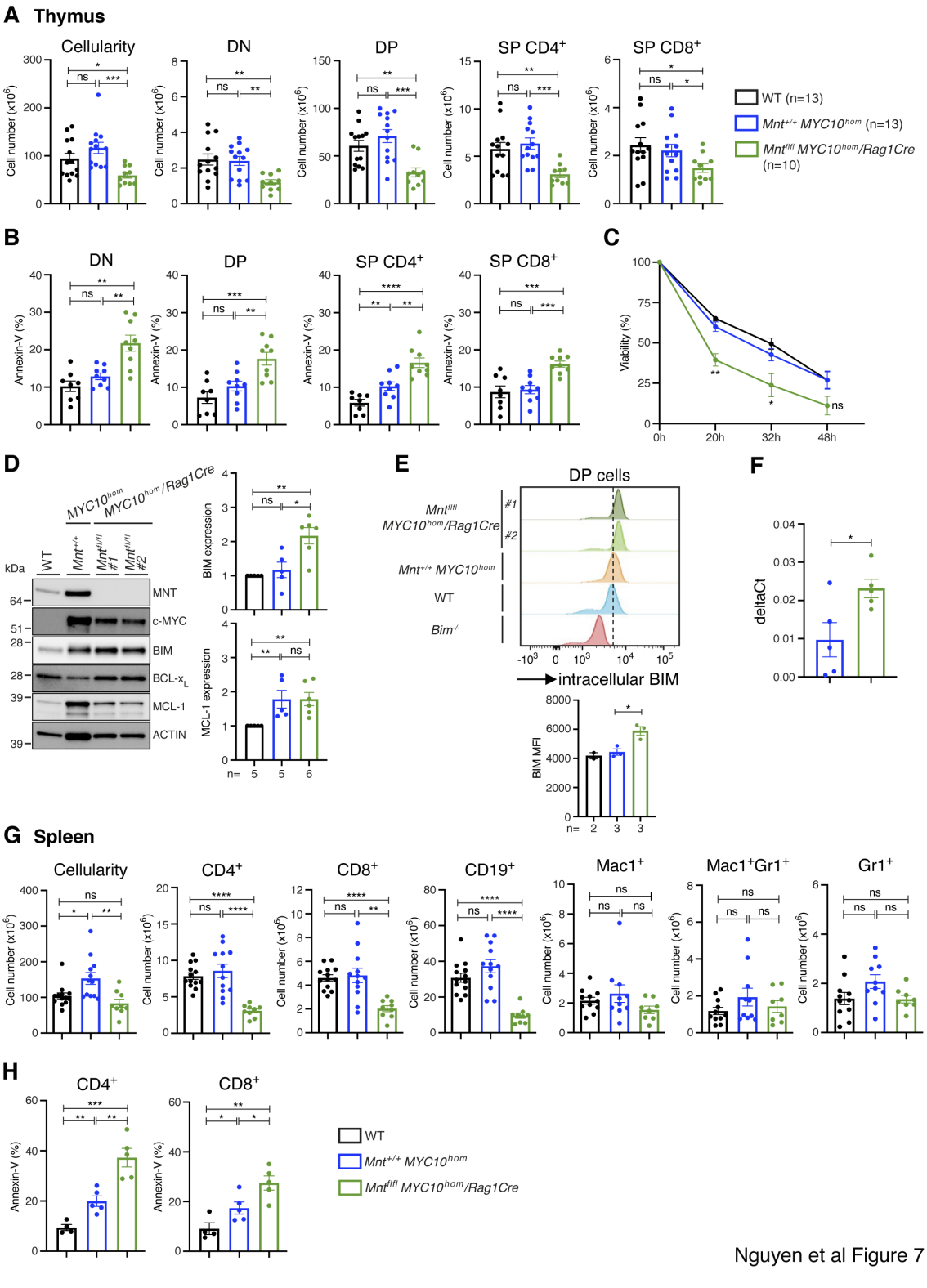

Figure 7

MNT loss impairs T cell development in premalignant *MYC10*^{hom} transgenic mice. Thymus (A-E): (A) Reduction in cellularity of all major thymic sub-populations in 8 wk-old premalignant *Mnt*$^{fl/fl}$*MYC10*^{hom}*/Rag1Cre* mice (green) versus premalignant *Mnt*$^{+/+}$*MYC10*^{hom} (blue) transgenic mice and control WT (black) mice. Cell number was determined by flow cytometry after immunostaining. (B, C) Elevated apoptosis of thymocytes in premalignant *MYC10*^{hom} transgenic mice is further enhanced by

MNT loss. (B) Quantification of AnnexinV-positive cells in major thymic sub-populations from WT (black), *Mnt*$^{+/+}$*MYC10*^{hom} (blue) and *Mnt*$^{fl/fl}$*MYC10*^{hom}*/Rag1Cre* (green) mice. (C) MNT loss enhances death of premalignant DP *MYC10*^{hom} thymocytes cultured *in vitro*. Sorted DP thymocytes were cultured at 37^{o}C in OptiMEM medium + 10% FCS and viability determined by PI staining at 0, 20, 32 and 48 hr. Values are expressed relative to viability at t=0. (D-F) MNT loss is associated with elevated BIM expression. (D) Left panel. Typical western blot showing elevated BIM levels in sorted DP thymocytes from 2 independent *Mnt*$^{fl/fl}$*MYC10*^{hom}*/Rag1Cre* mice versus control *Mnt*$^{+/+}$*MYC10*^{hom} or WT mice. Right panel shows quantification of BIM and MCL-1 protein in 2 independent western blots, normalized to ACTIN then to expression in WT cells (see Supplementary Fig. S7A for MNT, MYC and BCL-x_L quantification). (E) Elevated intracellular BIM staining in DP thymocytes from *Mnt*$^{fl/fl}$*MYC10*^{hom}*/Rag1Cre* versus control *Mnt*$^{+/+}$*MYC10*^{hom} mice. Upper panel shows a typical FACS analysis of intracellular BIM expression and lower panel presents BIM Mean Fluorescence Intensity (MFI) SEM for DP thymocytes from 2 independent WT and 3 independent *Mnt*$^{+/+}$*MYC10*^{hom} and *Mnt*$^{fl/fl}$*MYC10*^{hom}*/Rag1Cre* mice**.** DP thymocytes from *Bim*$^{-/-}$ mice served as a negative control. (F) Elevated *Bim* transcripts in DP thymocytes from *Mnt*$^{fl/fl}$*MYC10*^{hom}*/Rag1Cre* versus control *Mnt*$^{+/+}$*MYC10*^{hom} mice revealed by quantitative RT-PCR; values were calculated relative to *Gapdh* control. **Spleen (G, H):** (G) Marked reduction of T and B lymphoid but not myeloid cells in spleens of 8 wk-old premalignant MNT-null *MYC10*^{hom} transgenic mice. (H) Elevated apoptosis of splenic CD4^{+} and CD8^{+} T cells in MNT-null *MYC10*^{hom} transgenic mice, quantified by Annexin-V staining. Dots indicate individual mice, bars show mean SEM; * P£ 0.05, ** P £ 0.01; ***P £ 0.001, **** P £ 0.0001, ns = not significant.

Supplementary Files

This is a list of supplementary files associated with this preprint. Click to download.

- SupplementaryMaterialsandMethodsNguyenetal.docx
- LegendsforSupplementaryFigures.docx
- DistilledSupplementaryTables14.pdf
- FigS1Nguyenetal.tif
- FigS2Nguyenetal.tif
- FigS3Nguyenetal.tif
- FigS4Nguyen.tif
- FigS5Nguyen.tif
- FigS6Nguyen.tif
- FigS7Nguyen.tif
- FigS8Nguyen.tif
- FigS9Nguyen.tif